

)

SHAO SPECTROGRAPH FOR LOW-RESOLUTION SPECTRA

N. Z. Ismailov^{a*}, *S. A. Alishov*^a, *Sh. K. Ismailova*^a,
F. S. Huseinova^b

^a *N. Tusi Shamakhy Astrophysical Observatory of Azerbaijan National Academy of Sciences, Shamakhy, Azerbaijan*

^b *Batabat Astrophysical Observatory, Nakhichevan, Azerbaijan*

The paper describes an improved spectrograph of the Cassegrain focus of the 2 m SHAO reflector using a CCD camera. The classic Universal Astro Grid Spectrograph (UAGS) has been adapted to use the Andor CCD camera to obtain spectra of low-brightness objects in the range 3600–8000 Å. A spectrograph with a diffraction grating of 651 pcs/mm makes it possible to obtain spectra of stars on the 2 m SHAO telescope up to magnitude 18 with a resolution of $R = 1200$, with a signal to noise ratio of about 50 per half hour of exposure. The maximum allowed resolution is $R=3400$. The complex can be used to observe various types of transient objects, stars, and extragalactic objects.

Key words: astronomical instruments – spectrographs – CCD spectroscopy

1. DESCRIPTION OF THE SPECTROGRAPH

As is known, with the beginning of the use of CCD arrays in spectral observations, taking into account the compact dimensions of the light detector, in many observatories classical spectrographs were replaced by echelle spectrographs. When designing the echelle spectrograph at ShAO [1], the main goal was to obtain a high-resolution spectrum. With a 2 m telescope, such a spectrograph allows one to obtain spectra only of relatively bright objects. To carry out scientific work, it is often necessary to obtain spectra of radiation sources that are weak in brightness. Performing spectroscopy of faint stars and galaxies on telescopes of moderate and

⁾ AJAz:2023_2_54.pdf

* E-mail: ismailovnshao@gmail.com

medium size, with an aperture of 1–2 meters, is always an important observational task (see, for example, [2, 3]). To solve the above observational problem in the ShAO, we used the classical spectrograph UAGS (Karl Zeiss), which was previously used for photographic spectrophotometry (see, for example, [4, 5]). The spectrograph has been updated so that it can be used with modern CCD light detectors. To adapt the CCD to the spectrograph, a high-aperture Canon EF lens ($f=200$ mm, $f/2$) was used in the spectrograph camera. The remaining standard parts of the spectrograph were retained and adapted to this camera. The general view and optical scheme of the spectrograph are shown in Fig.1.

An Andor CCD camera (ikonL-936-BEX2-DD) (matrix 2048x2048, pixel size $13.5\mu\text{m}$) was used as a light receiver. The spectrograph is equipped with various classical diffraction gratings, which make it possible to obtain spectra in different ranges with different resolutions. The focal length of the collimator is $f_{\text{coll}} = 1100$ mm, the camera $f_{\text{cam}} = 200$ mm, the angles of incidence α and diffraction β are 27.5° and 20.5° , respectively. Then the width of the monochromatic image of the slit on the focal plane S' is determined by the relation

$$S' = S \frac{f_{\text{cam}} \cos \alpha}{f_{\text{coll}} \cos \beta}$$

Here S is the width of the entrance slit. Knowing the above parameters as a working formula for the input slot width S , we can obtain the following expression:

$$S = 5.275 S'$$

The receiver resolution element in the focal plane is equal to the size of two pixels, so for 1x1 binning the maximum width of the monochromatic image is $S' = 2\text{px} = 0.027$ mm, and accordingly, for the width of the entrance slit we obtain $S = 0.14$ mm. The equivalent focal length of the Cassegrain focus of a 2 m telescope is $F = 29500$ mm, and the scale is at the focal plane is $\mu = 6.99''/\text{mm}$. Then for the angular width of the entrance slit we get a value of $0.99''$, and when using the 2×2 pixel combining mode - $1.99''$. In order to simultaneously obtain the spectrum of the nearby background and the object, the slit height was set to about $10''$.

A diffraction grating with 651 pieces /mm was used, which at a blaze angle of 20.5° in the first order gives a spectrum with a linear inverse dispersion of about 144/mm in the range $\lambda 3600 - 8000 \text{ \AA}$. This is the most optimal combination of parameters for performing spectral observations of objects with low brightness. Table 1 lists the following parameters: entrance slit size $S(\text{mm})$; the size of the monochromatic image of the slit $S'(\text{mm})$ for a given binning; inverse linear dispersion in pixels $d(/\text{px})$; inverse linear dispersion $D(/mm)$; the corresponding

Table 1. Some spectrograph parameters

binning	S (mm)	S' (mm)	d (/px)	D (/mm)	$R(H\alpha)$
1x1	0.142	0.027	1.94	144	3400
2 × 2	0.285	0.054	3.89	288	1700
3 × 3	0.427	0.081	5.60	415	1170
4 × 4	0.570	0.108	7.56	560	870

spectral resolution $R = \lambda/\Delta\lambda$ in the region of the $H\alpha$ line for a given combination of parameters. From Table1 it can be seen that the best resolution can be obtained with a combination of binning 1×1 , with inverse linear dispersion $d = 1.9/\text{px}$. In other words, in the region of the $H\alpha$ line ($\lambda 6562.816$) in this mode we obtain a moderate spectral resolution, about $R = 3400$. With this resolution, the spectrum of a $V = 12$ mag star can be obtained in 15 minutes with a signal-to-noise ratio of about 50 .

2. OBSERVATION AND PROCESSING

2.1. Primary processing of observational material

We obtained many spectrograms of standard stars, as well as spectra of T Tauri and AeBe Herbig stars, etc. In addition, the spectra of various transient objects were obtained using this complex according the Gaia program (see, for example, [6,7]). During observations, you it is necessary to obtain 3 spectra of the star under study and standard stars, and then average them. Supporting frames flat, bias, dark were taken, as well as a comparison spectrum of the ThAr lamp for wavelength calibration. The Andor Solis 4.31 CCD camera control program allows you to change various parameters during observations, such as pixel binning mode, exposure time, operating mode, etc. The resulting spectra were further processed using the DECH20 program and its modifications (Galazutdinov G., <http://www.gazinur.com/DECH-software.html>).

The procedure for primary processing of spectral material is as follows: median frame averaging dark, bias, flat. Averaging of the resulting three images of the spectra of the program object and the spectra of standard stars. During the averaging process, the program simultaneously eliminates traces of cosmic radiation particles, which introduce a lot of distortion to the spectrum at long exposures. Subtraction of dark and bias frames from frames with spectra of observed objects. Construction of a mask that determines the position of the spectrum, its extraction using this mask, i.e. receiving a file in vector format *.200. The same procedure was performed for the flat field spectrum flat and the ThAr calibration

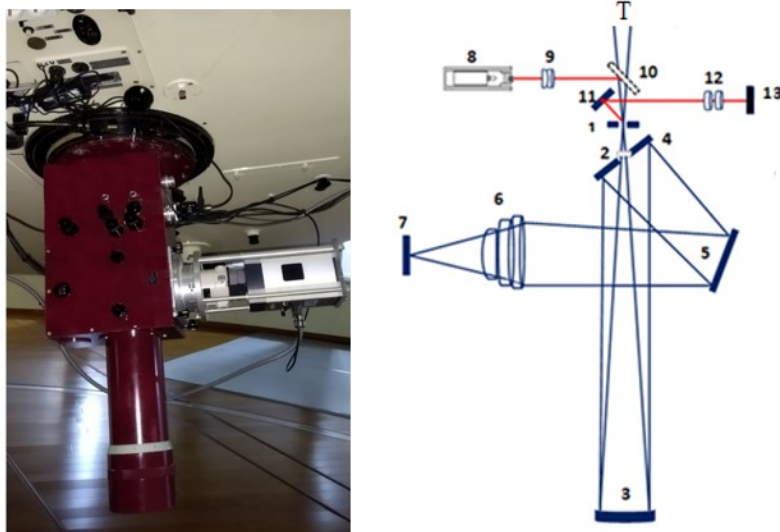


Fig. 1. General view and optical scheme of the spectrograph. The numbers indicate: 1-entrance slit, flat mirror 4 with hole 2, 3-collimator, 5-diffraction grating, 6-Canon camera, 7-CCD matrix window, 8-slit illumination lamp, 9-set of guide lenses, 10, 11 - folding mirrors, 12 - guide lenses for viewing the gap, 13 - monitor for tracking the slit.

lamp, which is needed for wavelength calibration. If, for some reason, during observations, not 3, but 2 spectra of a program star were obtained, then the extraction procedure is carried out without averaging, and only after the file extraction is completed and converted to the *.200 format, the resulting spectra are averaged. With this averaging, the program also cleans up non-repeating features in the spectrum, which mainly arise from cosmic particles.

2.2. Cleaning spectra from background illumination and light scattering of the spectrograph

Since in recent years there has been significant light pollution of the atmospheric background in the area where the ShAO is located, in spectrograms obtained with sufficiently long exposures details of this pollution are observed in the form of emission lines from mercury and other lamps and a weak continuum. This distortion is also supplemented by light scattering inside the spectrograph, which is distributed in a complex manner over the observed wavelength range and is superimposed on the spectrum of the observed object. The influence of the sky spectrum was taken into account in areas not illuminated by the light of the

observed star, thanks to the sufficient height of the slit (up to 10 arcseconds). As a result of this, in one image we get the spectrum of the object and the spectrum of the background below and above the spectrum of the object.

Figure 2 shows an example of inverted (negative) fits images for the resulting spectrum of classical T Tauri stars DI Cep (binning 1x1) and AS 205 (binning 2x2), where the spectrum of the star in the center and a wide spectrum of the background along the edges are highlighted. A bright line from mercury lamps $\lambda 5461$ is clearly visible in the spectra of the objects.

When extracting such a fits image, in addition to the main spectrum of the object, a mask is also built for the upper and lower background on each side. Using the resulting individual background and spectrum masks, you can obtain separate spectra of the background and object in *.200 vector format.

The average background spectrum is subtracted from the resulting spectrum, which makes it possible to clear background contamination and light scattering in the spectrograph. Figure 3 shows an example of the resulting *.200 file star+background, background and cleaned spectrum for Herbig Be type stars AS 310 . This procedure allows you to almost completely get rid of the background radiation and the radiation of scattered light from the spectrograph. Figure 4

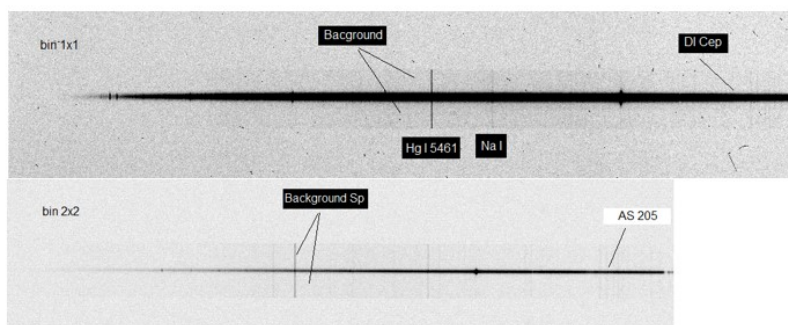


Fig. 2. Positive fits images of the spectra of classical T Tauri stars DI Cep (binning 1x1) and AS 205 (binning 2x2). The position of the Hg I and Na I lines from the background spectrum is noted

shows examples of the obtained spectrograms of two T Tauri stars DI Cep and AS205, and two Herbig AeBe stars AS310 and AS 442. The most intense lines are marked in the spectrum. And Fig. 5 shows parts of the spectra of these stars in the region $\lambda 4000 - 5000$. As can be seen from the spectrum, it is possible to measure the parameters of individual parts using the spectra.

2.3. Wavelength calibration

For wavelength calibration, spectra of the ThAr lamp, as well as spectra of standard stars with known radial velocities were used. When calibrating against the spectrum of a standard star, the reference points were set taking into account its radial velocities and barycentric speed of the Earth.

To evaluate the instrumental profile of the UAGS spectrograph, we measured the half-widths of the purest spectral lines from the spectrum of the ThAr calibration lamp. From about 10 lines selected, 2.20 ± 0.18 px were obtained for the half-width. With binning 1x1, such an instrumental contour is $\delta\lambda = 4.27 \pm 0.34$ Å. Figure 6 shows, for comparison, part of the spectra ($\lambda 4000 - 6700$) of dif-

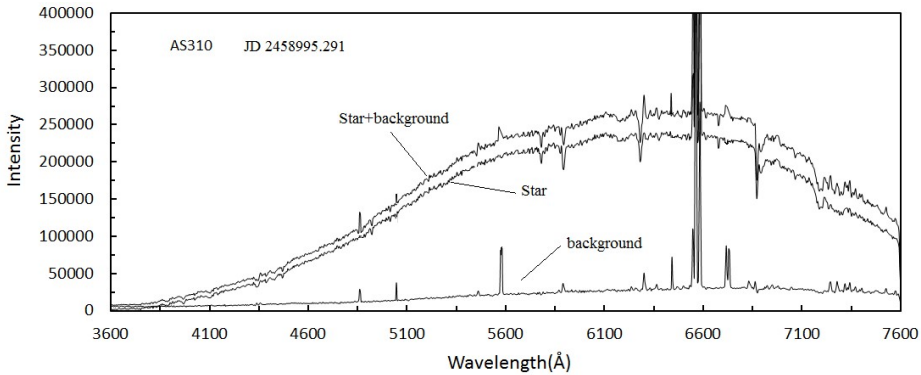


Fig. 3. Spectra from observation of the star AS 310: (Star+background) stars with background, (background) background, The star spectrum after clearing the parasitic background.

ferent stars obtained with our spectrograph, as well as the spectra of the same stars obtained with the 1.93 – m telescope of the Haute Provence observatory (ELODIE archive <http://atlas.obs-hp.fr/elodie/> [8]). The spectra of this archive can be convolved with an instrumental profile that is equal to the instrumental profile of our spectrograph. Our instrumental contour value is very close to the instrumental contour ~ 4.5 , which is given in [8]. The comparison showed that our spectra demonstrate good agreement with the compared spectra.

Figure [7] shows an example of a dispersion curve constructed in the DECH20 program from the spectrum of a ThAr lamp when approximated by a 3rd degree polynomial. The standard deviation of the positions of points near the reference lines from the polynomial curve is ± 0.008 mm (± 1.115). The errors in determining radial velocities for individual lines are $\pm 3 - 10$ km/s.

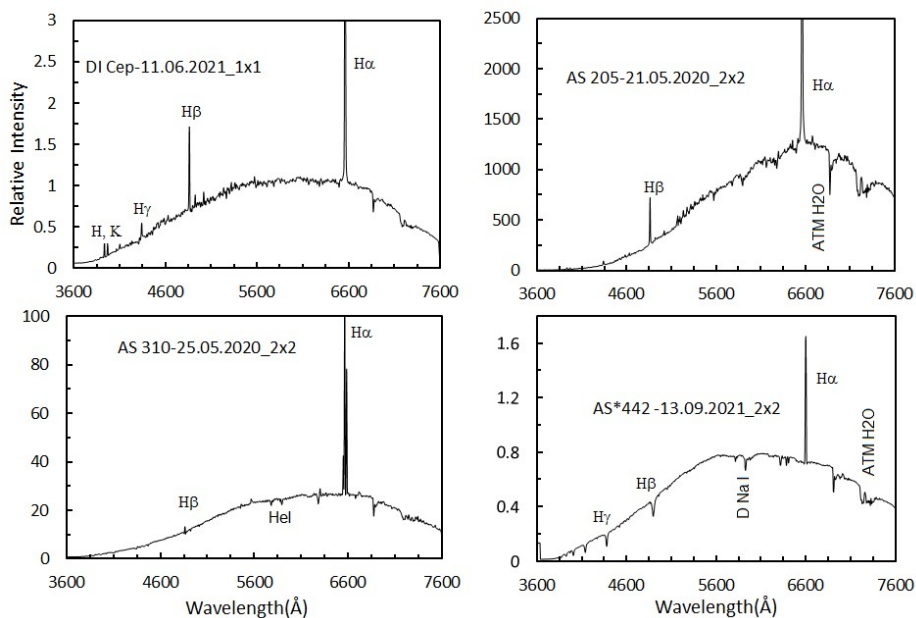


Fig. 4. Spectrograms of T Tauri stars DI Cep, AS 205, and Herbig AeBe stars AS 310 and AS 442. Text fields contain object names, spectrum acquisition dates, and binning.

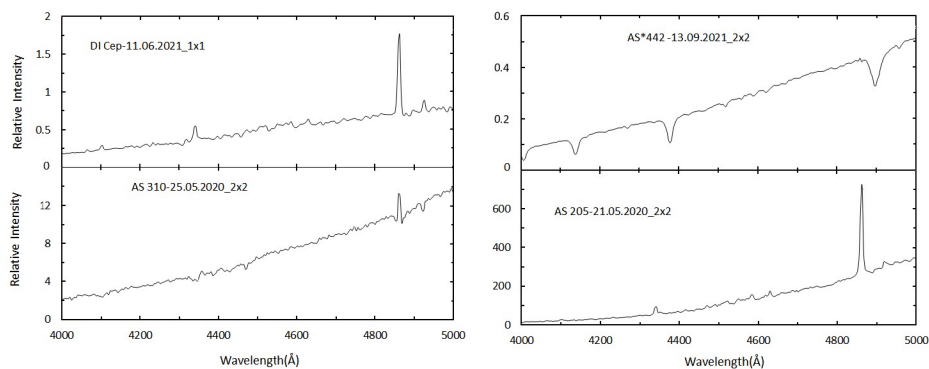


Fig. 5. Section (λ 4000-5000 Å) of the spectra of stars from Fig.4.

2.4. Measurement of some spectrophotometric parameters

The DECH program allows you to draw a continuum and perform spectrum normalization. After this procedure, the wavelength of the area is set and the required measurement of the spectrophotometric parameters of individual spectral lines is performed. The program also allows you to display spectrum data in digital form (ASCII), as wavelength-intensity, and it is also possible to save

individual sections of the spectrum as a file in BMP format.

The equivalent widths of the strongest hydrogen lines in stars of spectral class A0-A6 can be determined with an average error of $\pm 0.5 - 1.0$. Figure 8 shows an example of the results of measurements of equivalent widths EW of hydrogen lines $H\alpha - H8$ of the Balmer series based on the results of 6 nights of observations in August 2022 at the standard star 56 Cyg with an A6V spectrum. The standard deviation from the average EW does not exceed 10%. For comparison, in Fig. 8 on the right, large symbols show the results taken from [9] and [10] for a standard star with an A6 V spectrum. As can be seen, based on individual six nights of observations of the spectrum of 56 Cyg, our measurement results for the $H\gamma$, $H\delta$, and H8 lines are in satisfactory agreement with the data of [9, 10].

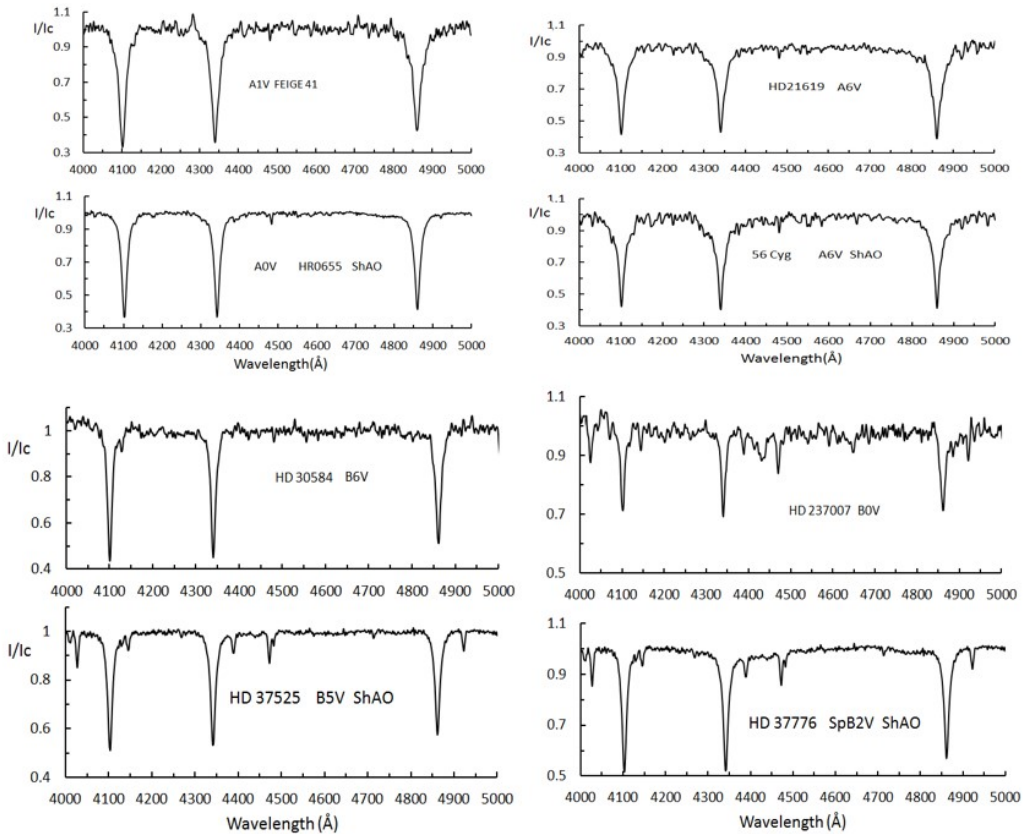


Fig. 6. Examples of normalized range $\lambda 4000-5000 \text{ \AA}$ for the spectra of different stars, given from the Vizer catalog [8] and obtained with our spectrograph. One of each pair of spectra of stars with similar spectral types was obtained at ShAO with the UAGS spectrograph with binning 1x1.

2.5. Expressing the spectrum in absolute fluxes

Since the entire spectrum of an object is obtained at the same order in classical linear form, transforming such a spectrum into absolute fluxes is not difficult. To express the spectrum in absolute fluxes, the hardware response curve (DQE) must be taken into account. To obtain an instrumental distortion for a given spectrum, it is necessary to obtain the spectrum of a standard star with a known distribution of the spectrum in absolute fluxes. In Fig. 9, as an example, we present the obtained instrumental spectrum of the standard star HR 0655 with spectral class A0V, and the equipment response curve of the DQE in this range.

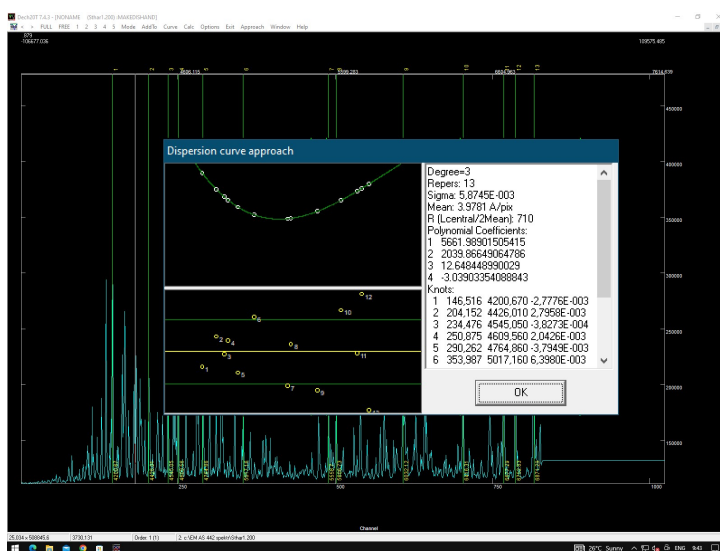


Fig. 7. An example of a plotted dispersion curve for the spectrum of a ThAr lamp in the DECH20 program window.

When the instrumental response curve is known, to transform the spectrum into absolute fluxes, the instrumental spectrum must be divided by the response curve and the spectral absorption due to the air mass must be taken into account. If, when obtaining the spectrum of the object under study, we simultaneously obtain the spectrum of a star with a known spectral distribution in absolute fluxes, which is located sufficiently close to the star, then the task of transformation into an absolute flux is significantly simplified. Figure 10 shows examples of spectra of various transient objects expressed in absolute fluxes. We published preliminary results of our studies of these stars in communications [6, 7].

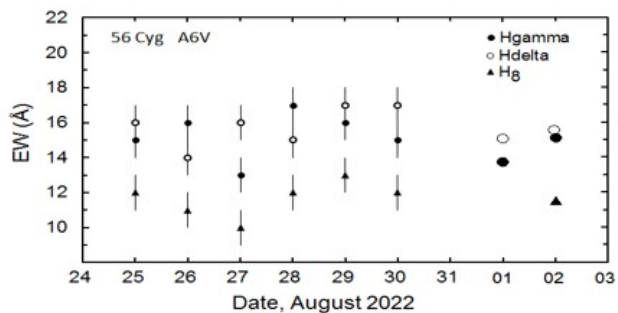


Fig. 8. The result of measurements of the equivalent widths of the Balmer lines $H\gamma$, $H\delta$ and $H8$ over 6 nights of observations in the spectrum of the standard star 56 Cyg. Vertical bars show the level of average measurement error. On the right, large individual symbols show the results taken from [9] and [10] for stars with A6V spectra.

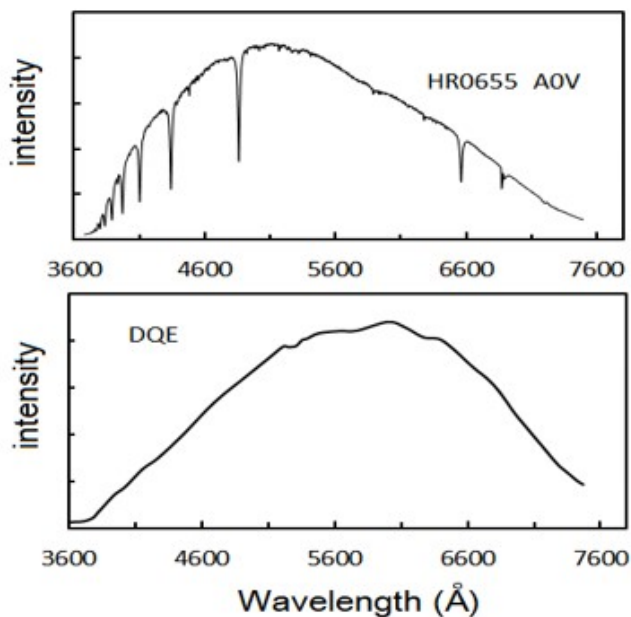


Fig. 9. An example of the instrumental spectrum of the standard star HR 0655 with an A0V spectrum (top panel) and an instrumental DQE curve for this spectral region.

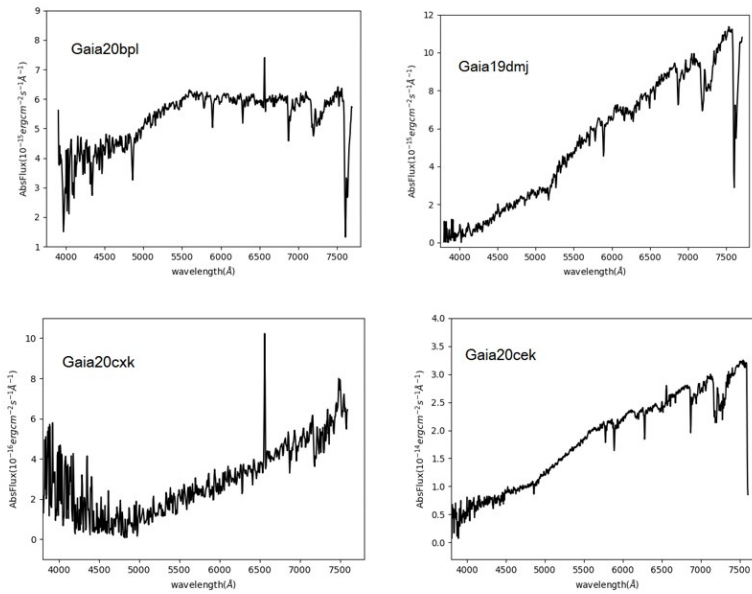


Fig. 10. Spectra of different transient Gaia objects, expressed in absolute fluxes.

3. CONCLUSION

Thus, the paper describes a modified classical UAGS spectrograph in combination with an Andor CCD camera. The device allows you to obtain spectra of objects with magnitude up to 18^{th} magnitude with a resolution of $R = 1200$ in the spectral range $\lambda 3600 - 8000$ in 60 minutes of exposure with signal to noise ratio is 20 . The best resolution in this system is $R = 3400$; with the binning parameters 1×1 and $R = 3400$ and with a signal-to-noise ratio of about 100 , the penetrating ability of the spectrograph on the 2 m SHAO reflector is about 15 magnitudes with an exposure of 30 minutes. A technique for purifying spurious radiation on the spectrum of a software object is described. The instrumental contour of the spectrograph was assessed and the profiles of different stars given in the literature and obtained at the ShAO were compared.

A technique for obtaining a spectrum in absolute fluxes is presented, which is important when studying the spectra of galaxies, quasars, supernovae and other transient objects. Examples of the spectra of some emission stars, expressed in absolute fluxes, are given. The spectra of standard stars show the magnitude of errors in measurements of equivalent widths and radial velocities. The spectrograph can be successfully used both for carrying out current planned scientific work and for carrying out various international cooperation.

4. ACKNOWLEDGMENTS

The authors thank the technicians and engineers of the 2 m telescope A. Ismailova, M. Shukyurova and I. Alekperova for their assistance in performing technical tasks to improve the spectrograph.

REFERENCES

1. Kh. M. Mikailov, F. A. Musaev, I. A. Alekberov, B. N. Rustamov, and O. V. Khalilov. *Kinematics and Physics of Celestial Bodies*, 2020, **36**, No. 1, 22.
2. V.L. Afanasiev, S.N. Dodonov, V.R. Amirkhanyan, A.V. Moiseev, *Astrophysical Bulletin*, 2016, **71**, 4, 479.
3. M.A. Nalivkin, I.S. Savanov, S.A. Naroenkov, V.E. Shmagin, *INASAN Science Reports*, 2019, **3**, 72 .
4. I.A. Aslanov, G.F. Sultanov, *Circular SHAO 1970*, No. 2, 3.,
5. G.F. Sultanov, *Circular SHAO 1970*, No. 2, 3.5.
6. I.R. Salmanov, *Circular SHAO 1975*, No. 44, 7.
7. I. Gezer, N.Z. Ismailov, Kh.M. Mikailov, O.V. Khalilov, I.A. Alekberov, S. Bagirli, S.A. Alishov, P.Zielinski, L.Wyrzykowski, M. Lam, K. Kruszynska, K.A. Rybicki, N. Ihanec, J. Zdanavicius, M. Maskoliunas, E. Pakstiene *The Astronomer's Telegram*, 2020, No. 13992.
8. P. Zielinski, L.Wyrzykowski, M. Lam, I. Gezer, K. Kruszynska, K.A. Rybicki, N. Ihanec, J. Zdanavicius, M. Maskoliunas, E. Pakstiene, N.Z. Ismailov, Kh.M. Mikailov, O.V. Khalilov, I.A. Alekberov, S.
9. Bagirli, S.A. Alishov *The Astronomer's Telegram*, 2020, 13907. G.H. Jacoby, D.A. Hunter, C.A. Christian, *Astrophys.J.Suppl.Ser.*, 1984, **56**, 257.
10. K.Cananzi, R. Augarde, J.Legueux. *Astron.Astrophys.Supple Ser.* 1993, **101**, 599.
11. R. M. Gonzalez Delgado, C. Leitherer, *Astrophys.J.Suppl.Ser.*, 1999, **125**, 479.